

Heteroepitaxial Recrystallization, a New Recrystallization Mechanism in Sub-Solvus Forged γ-γ' Nickel-Based Superalloys With Low Lattice Mismatch

Marie-Agathe Charpagne, Thomas Billot, Jean-Michel Franchet, Nathalie Bozzolo

▶ **To cite this version:**

Marie-Agathe Charpagne, Thomas Billot, Jean-Michel Franchet, Nathalie Bozzolo. Heteroepitaxial Recrystallization, a New Recrystallization Mechanism in Sub-Solvus Forged γ-γ' Nickel-Based Superalloys With Low Lattice Mismatch. 6th International Conference on Recrystallization and Grain Growth (ReX&GG 2016), Advanced Characterization, Testing, and Simulation Committee of the Structural Materials Division of The Minerals, Metals & Materials Society (TMS), Jul 2016, Pittsburgh, PA, United States. pp.259-264, 10.1002/9781119328827.ch38 . hal-01442527

HAL Id: hal-01442527

https://minesparis-psl.hal.science/hal-01442527

Submitted on 20 Jan 2017

HAL is a multi-disciplinary open access archive for the deposit and dissemination of scientific research documents, whether they are published or not. The documents may come from teaching and research institutions in France or abroad, or from public or private research centers.

L'archive ouverte pluridisciplinaire **HAL**, est destinée au dépôt et à la diffusion de documents scientifiques de niveau recherche, publiés ou non, émanant des établissements d'enseignement et de recherche français ou étrangers, des laboratoires publics ou privés.

HETEROEPITAXIAL RECRYSTALLIZATION, A NEW RECRYSTALLIZATION MECHANISM IN SUB-SOLVUS FORGED γ-γ' NICKEL-BASED SUPERALLOYS WITH LOW LATTICE MISMATCH

Marie-Agathe Charpagne[1,2] ; Thomas Billot[2]; Jean-Michel Franchet[3]; Nathalie Bozzolo[1]

[1] MINES ParisTech, PSL - Research University, CEMEF - Centre de mise en forme des matériaux, CNRS UMR 7635, CS 10207 rue Claude Daunesse 06904 Sophia Antipolis Cedex, France
[2] Snecma-Safran Group, Technical Department, 171 boulevard de Valmy – BP 31, 92702 Colombes Cedex, France
[3] Safran SA, SafranTech – Materials & Process Division, rue des Jeunes Bois – Châteaufort – CS 80112 78772, Magny-Les-Hameaux Cedex, France

Keywords: dynamic recrystallization, γ-γ' polycrystalline Nickel base superalloy, inverse precipitation

Abstract

A new dynamic recrystallization mechanism has recently been reported in γ-γ' Nickel-based superalloys after hot-forging in the sub-solvus domain. The mechanism leads to recrystallized grains encompassing a primary γ' precipitate having the same crystallographic orientation. The nucleation of those grains actually occurs before deformation by inverse precipitation of coherent γ phase at the rim of the primary γ' precipitates. This makes the specificity of that recrystallization process. Once the matrix starts being deformed, the coherent γ phase particles grow under the conventional stored-energy-consumption driving force. A detailed study of this new mechanism in the René65™ alloy has recently been published by the authors. Heteroepitaxially recristallized grains grow first, at low strain levels; then discontinuous dynamic recrystallization takes place, through classical necklace nucleation. Contrary to the usual trends for dynamic recrystallization kinetics, heteroepitaxial recrystallization goes faster with increasing strain rate and at lower temperatures. In the present paper, hot-forging experiments have been designed to demonstrate that the same mechanism can be triggered in other γ-γ' nickel base superalloys (Udimet 720 and RR1000).

Introduction

Dynamic recrystallization mechanisms and kinetics in polycrystalline Nickel base superalloys have been extensively studied in the past decades, notably because the grain size control is of utmost importance for high-technology hot-forged component made of those materials. Discontinuous recrystallization with nucleation on serrated grain boundaries has been established as the main mechanism governing microstructure evolution during deformation at high temperature [1–7]. If the alloy is forged in the γ' sub-solvus domain, primary γ' precipitates interact with grain boundaries of the recrystallized grains and limit their growth by the so-called Smith-Zener pinning phenomenon [8,9]. Consequently, the recrystallized grain boundaries typically end on those particles in the recrystallized microstructures. The present authors have recently reported the existence of another recrystallization mechanism referred to as *heteroepitaxial recrystallization*, which takes place in addition to conventional necklace

discontinuous dynamic recrystallization in the René65^{TM} superalloy. This new mechanism drastically contrasts with conventional ones by its nucleation process [10], its kinetics and its dependence on temperature and strain rate [10,11]. In the René65^{TM} alloy, the nucleation of such grains occurs when the material is slowly cooled from high temperature, typically at 5°C per minute. During slow cooling a complete or partial coherent γ shell forms around each γ' precipitate by inverse precipitation (γ'→γ). When such microstructure is further deformed at high temperature, the γ shells grow under the difference in stored energy with the surrounding matrix, and become heteroepitaxially recrystallized grains. This mechanism is the dominant recrystallization mechanism at low strain levels (typically $\varepsilon<0.6$). Since a low lattice mismatch between γ and γ' phases is a necessary condition for the development of such large heteroepitaxial features [12], the possible occurrence of heteroepitaxial recrystallization in other γ-γ' superalloys with low lattice mismatch is investigated in the present article.

Materials and processes

Two industrial γ-γ' superalloys have been selected for this study: Udimet 720 and RR1000 (composition given in Table 1). They both exhibit a low lattice mismatch : 0.02% for RR1000 [13], or even smaller for Udimet 720 [14]. Both of them initially presented a fine grain size of about 10 µm and contained primary γ' precipitates with a size in the range 1-3 µm. They were first submitted to a sub-solvus annealing treatment aiming at triggering the formation of γ shells around primary γ' precipitates. This treatment consists in a two-hours holding at a temperature T1 and slow cooling down to a temperature T2 at 5°C.min^{-1} and then air cooling from T2 to room temperature. The temperatures T1 and T2 (given in Table 2) were adjusted relative to the γ'-solvus temperature of each alloy.

wt (%)	Al	Ti	Co	Cr	Mo	Zr	Hf	Ta	B	W	C	Ni
RR1000	3.0	3.6	18.5	15.0	5.0	0.06	0.5	2.0	0.015	-	0.027	bal.
Udimet 720 [15]	2.5	5.0	14.7	18.0	3.0	0.03	-	-	0.033	1.25	0.035	bal.

Table 1: Nominal composition of RR1000 and Udimet 720 alloys

Alloy	T1 (°C)	T2 (°C)
Udimet 720	1050	600
RR1000	1095	745

Table 2: Temperatures of the annealing treatment for each superalloy

Following this thermal treatment, cylindrical Udimet 720 samples (6 mm in diameter, 9 mm in height) were deformed by hot-compression up to a height reduction of 2:1 under the following conditions: 1000°C-0.1s^{-1}; 1040°C-0.1s^{-1} and 1040°C-0.01s^{-1}. All samples were mechanically polished using diamond suspensions down to 1 µm in size and characterized using the coupled EDS-EBSD method described in [12] that allows for separating primary γ' precipitates from the γ matrix . Microstructure was characterized at the center of the deformed samples, where the strain level is the highest.

Results and discussion

1. Annealed samples

Fig. 1 presents the microstructure of the annealed RR1000 sample within various imaging modes. The Forward Scattered Electron (FSE) image of Fig. 1-a reveals both topographic and crystallographic contrasts [16], and thus allows for highlighting the location of γ' precipitates as they were slightly dug during polishing. Fig. 1-b to Fig. 1-d are different plots of the

corresponding EBSD map: the trace of the precipitates itself is hardly visible on the Pattern Quality (PQ) map (Fig. 1-b), but a γ grain boundary encircles each precipitate. Fig. 1-c confirms the presence of a γ shell around the precipitates, having the same crystallographic orientation as the precipitate. No significant orientation variation can indeed be revealed either at the γ-γ' interface on the Kernel Average Misorientation (KAM) map of Fig. 1-d.

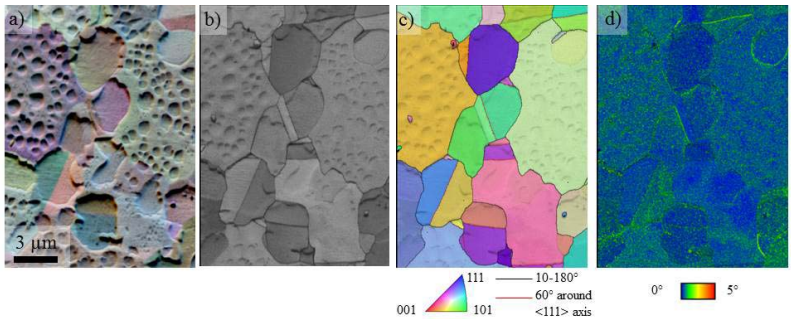


Figure 1: Annealed RR1000 superalloy. a) FSE image; b-d) corresponding EBSD maps of the same area (step size: 37 nm): b) PQ map; c) Orientation map within a color code indicating which crystallographic direction is parallel to the normal to the scanned section; d) KAM map (average misorientation angle between each pixel and its first neighbours, excluding disorientations higher than 5°).

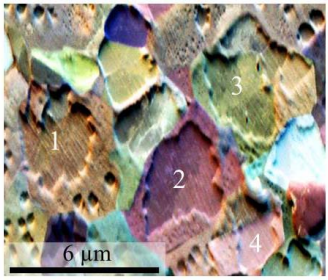


Figure 2: FSE image of the annealed Udimet 720 sample.

The FSE image of the annealed Udimet 720 sample (Fig.2) shows similarities with Fig.1-a. The primary γ' precipitates numbered 1 to 4 are surrounded by a coherent γ shell.

The microstructures of Figs. 1 and 2 are actually typical of materials having undergone the inverse precipitation process originally described in [10,11] for the René65^{TM} alloy. In order to check whether those coherent γ shells can lead to hetero-epitaxial recrystallization in those alloys as well, three Udimet 720 samples have been deformed in the sub-solvus domain, as presented below.

2. Udimet 720 samples after hot-compression

An EBSD map of the sample deformed at 1000°C and $0.1s^{-1}$, color coded according to the Grain Orientation Spread (GOS) value, is presented on Fig. 3. The black areas correspond to the primary γ' precipitates, filtered out thanks to the use of EDS combined with EBSD [12].

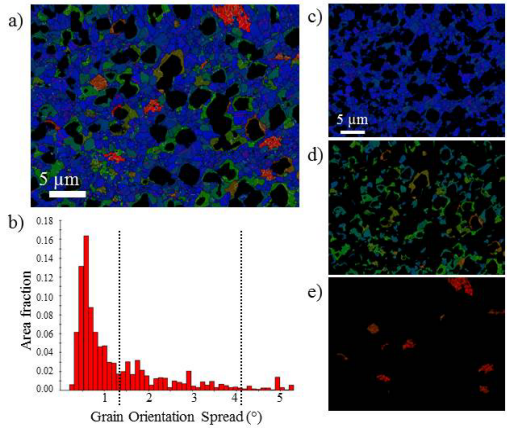


Figure 3: Udimet 720 sample after annealing treatment and subsequent deformation at 1000°C and $0.1s^{-1}$, followed by water quenching. a) GOS map of the γ matrix with primary γ' precipitates plotted black, b) GOS distribution histogram, c) grains appeared by discontinuous dynamic recrystallization (GOS<1.2°), d) heteroepitaxially recrystallized grains (1.2°<GOS<4.1°), e) non-recrystallized matrix grains (GOS>4.1°). Grain boundaries (>10°) in black and twin boundaries (60°<111>, with a tolerance of 5°) in red.

Fig.3-a enables to identify three populations of grains, reported on the associated GOS distribution of Fig.3-b, and shown separately on Figs.3-c to 3-e. The dominant population appears in blue color (GOS<1.2°, Fig.3-c). Those grains have the lowest internal misorientations in the microstructure, i.e. those are the grains with the lowest dislocation content. From this observation, one can conclude that those grains have formed late in the dynamic recrystallization process. A second population with higher internal misorientations is highlighted on Fig.3-d (1.2° < GOS < 4.2°). Those grains have a shape of rings, or parts of rings, as they embed a primary γ' precipitate. Their higher GOS value suggests that they have formed before the former population of Fig.3-c and have been subsequently deformed, storing dislocations before deformation ended. Finally, few grains with significantly higher internal misorientations (thus higher dislocation density) also remain in the microstructure (red grains of Figs.3-a and 3-e). Those are matrix grains which were present in the initial microstructure and have not recrystallized yet.

By using a double thresholding on the GOS distribution and considering the shape and size of the recrystallized grains, two recrystallized populations could thus be identified, and their apparition relatively to each other in the recrystallization process could be deduced from their average GOS value, indicative for the dislocation content. The nature of those recrystallized populations can be further detailed by analyzing their orientation and location in the microstructure.

Fig. 4 presents the deformed microstructure of Fig. 3 within other imaging modes. From the comparison of Fig.4-a and Fig.4-b, among the recrystallized grains, those with the highest internal misorientations appear to be heteroepitaxially recrystallized grains. As clearly visible on Fig.4-a and 4-dc and confirmed on the BackScattered Electron (BSE) image of Fig.4-d, they

embed a primary γ' precipitate having the same crystallographic orientation (see the typical example highlighted on all images). Those grains arise from the coherent γ shell, which has formed during the cooling stage of the annealing treatment performed prior to deformation. On the other hand, the other population of recrystallized grains, small equiaxed grains with low internal misorientations shown of Fig. 3-d, has no specific orientation. It arose from the conventional necklace dynamic recrystallization mechanism.

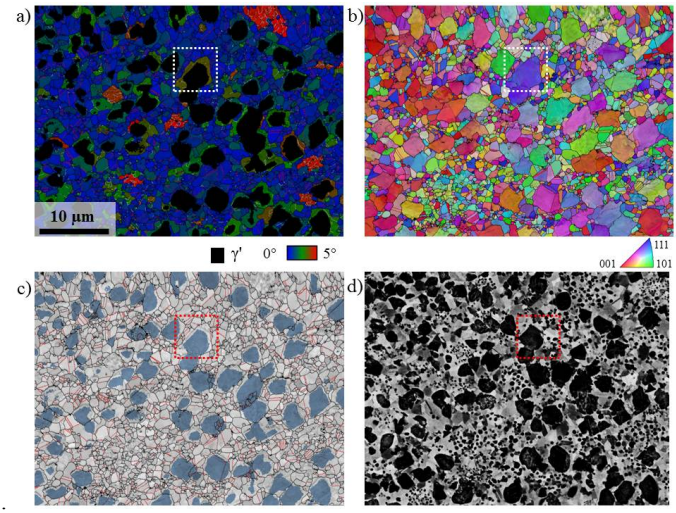


Figure 4: Same sample as Fig.3. a) GOS map of the γ matrix with primary γ' precipitates plotted black, b) Orientation map within a color code indicating which crystallographic direction is parallel to the normal to the scanned section, c) pattern quality superimposed with EDX-resolved phase map (primary γ' precipitates in blue color), d) BSE image

In order to check whether the evolution trends of the heteroepitaxially recrystallized grains with temperature and strain rate are similar to those obtained in the René65^{TM} superalloy [10], the microstructure of two other samples deformed under different conditions was investigated using similar GOS thresholding. Table 3 displays the obtained area fraction and average grain size for all three grain populations depicted in Fig. 3.

	1000°C 0.1s^{-1}	1040°C 0.1s^{-1}	1040°C 0.01s^{-1}
Classical dynamically recrystallized grains	*0.67* - 1.0 µm	*0.68* - 1.3 µm	*0.65* - 2.3 µm
Hetero-epitaxially recrystallized grains	***0.30* - 1.3** µm	***0.24* - 1.5** µm	***0.21* - 2.3** µm
Deformed matrix grains	*0.03* - 2.1 µm	*0.08* - 1.9 µm	*0.14* - 5.0 µm

Table 3: Area fraction *f* and equivalent circle diameter (µm) of the two types of recrystallized grains and of the non-recrystallized grains in Udimet 720 after annealing and compression under different conditions

The recrystallized grain size slightly increases with temperature both types of recrystallized grains (see both samples deformed at 0.1s^{-1}). The area fraction of heteroepitaxially recrystallized grains is higher: at 0.1s^{-1} (the highest strain rate) at 1040°C, and at 1000°C (the lowest

temperature) at $0.1s^{-1}$. Those results are fully consistent with the tendencies observed in the René 65 superalloy [10,11] and can be explained by the balance between two opposite driving forces: first the difference in stored energy which promotes the growth of the heteroepitaxially recrystallized grains against the surrounding matrix ; second, the difference in chemical potential of the γ-gene elements across the γ'-γ interface, which tends to dissolve the γ shells back into the precipitates since the deformation temperature is higher than the temperature at which inverse precipitation occurred during the former cooling stage.

Conclusion

This article demonstrates that heteroepitaxial recrystallization, observed first in René 65 superalloy, also occurs in at least two other superalloys with a low lattice mismatch: RR1000 and Udimet 720. A rough investigation of the deformation conditions promoting hetero-epitaxial recrystallization in Udimet 720 leads to the same conclusions than in the René 65 alloy. This mechanism is intensified at low temperatures and high strain rates, which is opposite to the tendencies of classical discontinuous dynamic recrystallization. Taking this mechanism into account is crucial when aiming at describing accurately the softening processes which take place during forging and the resulting microstructures.

References

[1] G. Shen, S.L. Semiatin, R. Shivpuri, Modeling microstructural development during the forging of Waspaloy, Metall. Mater. Trans. A. 26 (1995) 1795–1803. doi:10.1007/BF02670767.

[2] S.. Medeiros, Y.V.R.. Prasad, W.. Frazier, R. Srinivasan, Microstructural modeling of metadynamic recrystallization in hot working of IN 718 superalloy, Mater. Sci. Eng. A. 293 (2000) 198–207. doi:10.1016/S0921-5093(00)01053-4.

[3] Q. Guo, D. Li, S. Guo, H. Peng, J. Hu, The effect of deformation temperature on the microstructure evolution of Inconel 625 superalloy, J. Nucl. Mater. 414 (2011) 440–450. doi:10.1016/j.jnucmat.2011.05.029.

[4] S. Mitsche, C. Sommitsch, D. Huber, M. Stockinger, P. Poelt, Assessment of dynamic softening mechanisms in Allvac® 718Plus™ by EBSD analysis, Mater. Sci. Eng. A. 528 (2011) 3754–3760. doi:10.1016/j.msea.2011.01.044.

[5] B. Lindsley, X. Pierron, Sub-solvus recrystallization mechanisms in UDIMET (R) alloy 720LI, SUPERALLOYS 2000. (2000) 59–68.

[6] H. Zhang, K. Zhang, S. Jiang, H. Zhou, C. Zhao, X. Yang, Dynamic recrystallization behavior of a γ′-hardened nickel-based superalloy during hot deformation, J. Alloys Compd. 623 (2015) 374–385. doi:10.1016/j.jallcom.2014.11.056.

[7] Y.C. Lin, X.-Y. Wu, X.-M. Chen, J. Chen, D.-X. Wen, J.-L. Zhang, et al., EBSD study of a hot deformed nickel-based superalloy, J. Alloys Compd. 640 (2015) 101–113. doi:10.1016/j.jallcom.2015.04.008.

[8] M. ASHBY, J. HARPER, J. LEWIS, INTERACTION OF CRYSTAL BOUNDARIES WITH SECOND-PHASE PARTICLES, Trans. Metall. Soc. AIME. 245 (1969) 413–&.

[9] C.S. Smith, Zener pinning, Trans. Met. Soc. AIME. 175 (1948) 15–51.

[10] M.-A. Charpagne, T. Billot, J.-M. Franchet, N. Bozzolo, Hereroepitaxial recrystallization: a new mechanism simultaneous to conventional discontinuous dynamic recrystallizaton, discovered in a polycristalline γ-γ' nickel-based superalloy, Submitted. (2016).

[11] M.-A. Charpagne, T. Billot, J.-M. Franchet, N. Bozzolo, Heteroepitaxial recrystallization observed in René 65 and Udimet 720: a new recrystallization mechanism possibly occuring also in other low lattice mismatch γ/γ' Nickel-based superalloys, in: Submitt. to Superalloys 2016, TMS, 2016.

[12] M.-A. Charpagne, P. Vennéguès, T. Billot, J.-M. Franchet, N. Bozzolo, Evidence of multimicrometric coherent γ' precipitates in a γ-γ' Nickel-based superalloy, J. Microsc. (2016). http://onlinelibrary.wiley.com/doi/10.1111/jmi.12380/full.

[13] B.M.B. Grant, E. Knoche, M. Preuss, J. Quinta da Fonseca, M.R. Daymond, The Effect of Lattice Misfit on Deformation Mechanisms at High Temperature, Adv. Mater. Res. 278 (2011) 144–149. doi:10.4028/www.scientific.net/AMR.278.144.

[14] R.A. Ricks, A.J. Porter, R.C. Ecob, The growth of γ′ precipitates in nickel-base superalloys, Acta Metall. 31 (1983) 43–53. doi:10.1016/0001-6160(83)90062-7.

[15] F.E. Sczerzenie, G.E. Maurer, Development of Udimet 720 for High Strength Disk Applications, (1984) 573–580.

[16] A. Day, Developments in the EBSP technique and their application to grain imaging, Ph. D. dissertation, University of Bristol, 1993.